UCRL-JC--108019

DE92 002180

Enhanced Lower Hybrid Penetration via Intense Multi-Microsecond Pulses

R.H. Cohen
T.D. Rognlien
P.T. Bonoli
M. Porkolab

THIS PAPER WAS PREPARED FOR SUBMITTAL TO
9th Topical Conference on
Radio Frequency Power in Plasmas

Charleston, South Carolina

August 19-21, 1991

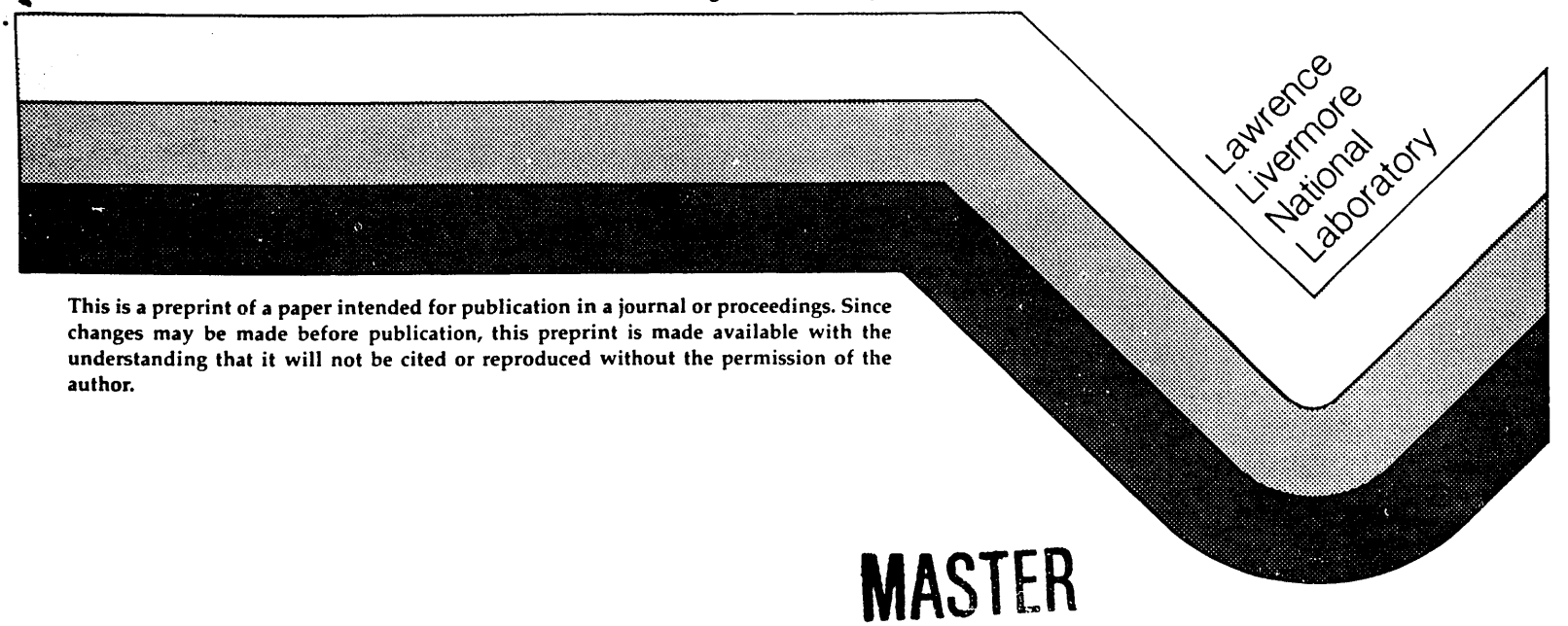

DISCLAIMER

ENHANCED LOWER HYBRID PENETRATION VIA INTENSE MULTI-MICROSECOND PULSES

R. H. Cohen, T. D. Rognlien
Lawrence Livermore National Laboratory, University of California
Livermore, California 94550 USA

P. T. Bonoli, M. Porkolab
Plasma Fusion Center, Massachusetts Institute of Technology
Cambridge, Massachusetts 02139 USA

ABSTRACT

Applying lower-hybrid power in short, intense pulses can overcome Landau damping, allowing penetration into the core of reactor-grade plasmas. We present a theoretical description of the absorption which accounts for transient collisional effects as well as nonlinear broadening of the resonant plateau. We show results from ray-tracing calculations which include the nonlinear absorption. We also derive the conditions required for pump depletion by parametric instabilities, and assess density depletion by ponderomotive effects, scattering by low-frequency background fluctuations, and filamentation. Consideration of all of the aforementioned effects as well as potential source availability and launcher requirements leads to the consideration of scenarios based on 5-10 GW 30-100 μs pulses for the ITER Conceptual Design. Experimental tests of the concept can be done by launching waves with high enough parallel wavenumber that the resonant electrons are only moderately far out on the tail of the distribution function. The experiments would entail checking the predicted variation of the penetration with the duration and peak power of the pulses as well as the launcher area. We give sample experimental parameters for the Microwave Tokamak Experiment (MTX), Alcator C-Mod, Versator, and DIII-D.

INTRODUCTION

Lower-hybrid waves are a proven means of heating and driving current in tokamak plasmas. Hence they provide a potential route to the creation of a steady-state tokamak. Unfortunately, conventional (CW) lower-hybrid waves tend to be excluded from the interior of reactor-grade tokamak plasmas because waves which could exist in the core (those which satisfy the accessibility condition) are strongly Landau-damped on the way in. This has been confirmed by recent numerical studies[1]. However, application of lower-hybrid power in short, intense pulses enhances penetration by saturating the power absorbed through Landau damping[2]. For a device such as the International Thermonuclear Experimental Reactor (ITER)[3], we envision multi-GW peak, 100-200 MW average power at 8-10 GHz driving 10-20 MA of d.c. current. Ref. 2 gave a partial theoretical description of the absorption and parametric stability of very short (10's of ns) pulses, such as might be obtained from an induction-linac-driven relativistic klystron ("regime A"). We have since found that there are significant advantages to operating with longer pulses ("regime B"), with durations τ_p comparable to the collisional relaxation time τ_r of the nonlinear plateau (of width Δu in parallel velocity u). A brief description of a theory of the nonlinear absorption and ray-tracing results for this regime, as well as description of parametric instabilities valid in either regime, was presented in Ref. 3. Here, we provide a more extended account of the absorption physics, review the ray-tracing and parametric-instability calculations, and discuss new

calculations applying the results of the theory to competing ITER designs and possible near-term tests on several tokamaks.

ABSORPTION

The nature of the absorption depends on the pulse duration τ_p. For a narrow spectrum of wave phase velocities $\omega/k_\parallel$ and for $\tau_p << \tau_r$, the dominant energy absorption process is the collisionless mixing of the distribution function in the neighborhood of the Landau resonance, as a result of trapping oscillations; the result is the creation of the nonlinear plateau, whose width is approximately the maximum width of the separatrix bounding trapped electrons in phase space. The plateau is further broadened by a spread in $\omega/k_\parallel$. The absorbed power is dominated by the energy $\mathcal{E}_0$ required to initially create the plateau in the absence of collisions (See Fig. 1). This regime in

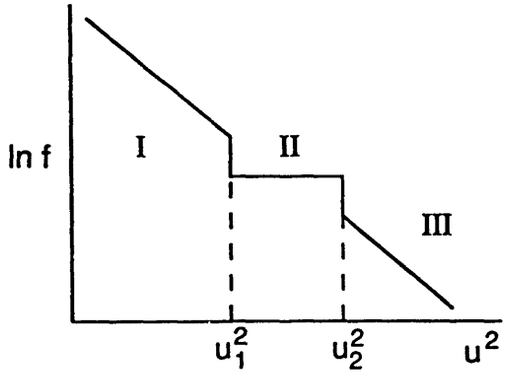

Fig. 1. Sketch of distribution function showing collisionless plateau

turn has a multitude of sub-regimes, of which three are of potential interest for our applications: for τ_p long compared to the trapping period of a resonant electron but short compared to the transit time across the microwave beam, $\mathcal{E}_0$ is independent of τ_p so that $\langle P\rangle$, the power absorbed averaged over the duration and cross-sectional area (along a flux surface) of the beam, satisfies $\langle P\rangle \propto \tau_p^{-1}$. For τ_p long compared to the beam-transit time but short compared to τ_{fs}, the time for all electrons on a flux surface to pass through the microwave beam, then $\mathcal{E}_0 \propto \tau_p$ so that $\langle P\rangle = \text{const}$. Finally, for $\tau_{fs} << \tau_p << \tau_r$, $\mathcal{E}_0$ is again independent of τ_p so that $\langle P\rangle \propto \tau_p^{-1}$ (but with a coefficient smaller by the ratio of the area of the beam to the area of the flux surface than for the first sub-regime). This is the sub-regime of interest for the present paper. Defining the absorption coefficient $\alpha = \langle \mathcal{S}^{-1} d\mathcal{S}/ds\rangle$, where $\mathcal{S}$ is the r.f. energy flux normal to a magnetic surface and s denotes length along a ray projected into the poloidal cross section, we obtain, for this sub-regime,

$$\alpha = \alpha_0 \equiv \frac{nA_\psi}{A_b\mathcal{S}}\frac{T_e v_t H e^{-\epsilon_1}}{2\pi^{1/2}u_r\tau_p} \tag{1}$$

where $\epsilon = \mathcal{E}_\parallel/T_e$, A_ψ and A_b are the areas of the flux surface and the projection of the beam onto it, respectively, $H = e^{\epsilon_1}(u_r/3v_t)\left[2K\Delta(\tilde{u}^3) - 3K\Delta\tilde{u} + 3\Delta\left(\tilde{u}e^{-\epsilon}\right)\right]$, $\Delta x \equiv x_2 - x_1$ with 1 and 2 denoting values at either side of the plateau, $\tilde{u} = u/v_t$, and $K = \pi^{1/2}(2\Delta\tilde{u})^{-1}\Delta\left(\text{erf}\,\epsilon^{1/2}\right)$. The first and second sub-regimes are recovered (approximately, in the latter case) by replacing A_ψ by A_b and $hu_r\tau_p$, respectively, where h is the beam height across field lines.

The originally proposed[2] scenario, motivated by the development of relativistic klystrons and other short-pulse sources, was described primarily by the second of the

above sub-regimes. Because of the strong dependence of the absorption coefficient on plateau width [$\propto (\Delta u)^3$ for small Δu] and the dependence of the plateau width on r.f. flux density (see below), the absorption coefficient decreases slowly with applied power, leading to the requirement of $\sim$ 100 GW pulses for good penetration in ITER. Even then, the power has to be launched from structures narrow transverse to the magnetic field and highly elongated along it, in order to simultaneously minimize the number of electrons passing through the beam and the r.f. flux density. The design of such launchers is a difficult engineering feat even for a single, known magnetic equilibrium. Furthermore, criteria for avoidance of parametric decay instabilities, while most easily satisfied for the same elongated launching structures, are at best marginally satisfied. These factors motivate the consideration of longer pulses (third sub-regime), where the launcher shape is no longer a factor (all electrons pass through the beam) and the pulse-averaged absorption coefficient α_0 decreases with τ_p. The primary question is then the determination of collisional effects which limit the improvement with increased τ_p.

The collisional dissipation consists of two pieces: a transient boundary-layer contribution that removes the discontinuities in the distribution function at either end of the collisionless plateau, and a steady-state relaxation toward Maxwellian of the constantly-regenerated plateau. Assuming that the time t_s to set up the nonlinear plateau ($\sim$ the trapping period for a narrow spectrum of phase velocities) is short compared to the collisional relaxation time of the plateau, then, for $\tau_p >> t_s$, we have $\alpha = \alpha_0 + \alpha_{bl} + \alpha_{ss}$, where α_t and α_{ss} are the contributions from the transient boundary layers and from the steady-state dissipation of the plateau, respectively. For small $\Delta u/u$, the dissipation can be calculated by a boundary-layer analysis of a one-dimensional Fokker-Planck equation (obtained by assuming that the perpendicular variation is Maxwellian) which can be written in the form[4]:

$$\frac{\partial F}{\partial t} = \mathcal{D} + \hat{\nu}\frac{\partial}{\partial u}\left[\frac{T_e}{m_e u^3}\frac{\partial}{\partial u} + \frac{1}{u^2}\right] F \qquad (2)$$

where $\mathcal{D} = -\partial\Gamma_{rf}/\partial u$ is the r.f. operator and the flux Γ_{rf} need not be diffusive, F is the electron distribution function integrated over perpendicular velocity, $\hat{\nu} = (2+Z)\nu v_t^3$, $v_t = (2T_e/m_e)^{1/2}$, and $\nu = 4\pi n_e e^4 \Lambda/m_e^2 v_t^3$ with Λ the Coulomb logarithm, and Z is the effective charge state. The analysis proceeds as follows: divide u space into regions as shown in FIg. 1, and consider $\mathcal{D}$ to be zero in regions I and III but dominant in region II, so that $F_{II} \approx$ constant. The r.f. power dissipated is $P = \int d^3v\, mu\Gamma_{rf}$. Solving Eq. (2) in region II by ordering in inverse powers of $\mathcal{D}$, we find that $\Gamma_{rf} \approx \hat{\nu}F_0/u^2 + C$, where F_0 is the value of the zero-order (plateau) F in region II and the integration constant C is the collisional flux across the boundary of regions I and II, $C = -\hat{\nu}\left[(F/u^2) + (T/mu^3)\partial F/\partial u\right]_{u_1^-}$. In the expression for Γ_{rf}, the F_0 piece leads to α_{ss}, while C generates the transient contribution α_{bl}. We solve for C by switching variables in Eq. (2) from u to the parallel energy $\mathcal{E}_\parallel$, introducing $g = F\exp(\mathcal{E}_\parallel/T_e)$, treating as constant the coefficients of the $\mathcal{E}_\parallel$ derivatives of g, and then Laplace transforming the resulting equation in time. The result is two coupled boundary-layer problems for regions I and III, connected via F_0 and its time derivative. Solving, we find

$$\alpha_{\rm bl} = \frac{nA_\psi}{A_b\mathcal{S}}\frac{\tilde{\nu}\Delta\mathcal{E}_\parallel\Delta e^{-\epsilon}}{\pi\epsilon^{3/4}(2\hat{\nu}\tau_p)^{1/2}} \qquad \text{and} \qquad \alpha_{\rm ss} = \frac{nA_\psi}{A_b\mathcal{S}}\tilde{\nu}T\ln(u_2/u_1)\frac{\Delta(\mathrm{erf}\,\epsilon^{1/2})}{\Delta u} \quad , \qquad (3)$$

where $\tilde{\nu} = \nu(2+Z)$. The result for $\alpha_{\rm ss}$ is equivalent to that obtained by Fisch[5]. For narrow plateaus, α_0, $\alpha_{\rm bl}$ and $\alpha_{\rm ss}$ scale as the third, second, and first powers of the

plateau width,respectively. Note that α_{bl} and α_{ss} become equal for $\tau_p \approx (2/\pi)\nu^{-1}(2+Z)^{-1}\epsilon^{5/2}(\Delta u/u)^2$, which is a fraction of the plateau relaxation time, while the collisionless term α_0 is small. This choice of τ_p is a good compromise between penetration and source technology considerations. A generalization of Eqs. (1) and (3) to relativistic parallel dynamics is straightforward and will be described elsewhere; the most important relativistic corrections are captured by using the relativistic energy in Eqs. (1) and (3), which we do in the ray-tracing calculations described below.

A sample comparison between the analytic expression for the power absorbed, $P_a = \alpha A_b \mathcal{S}$, and the numerical result from the Fokker-Planck code CQL[6] is shown in Fig. 2. We compare a nonrelativistic case with the following parameters: $n_e = 1 \times 10^{20}$

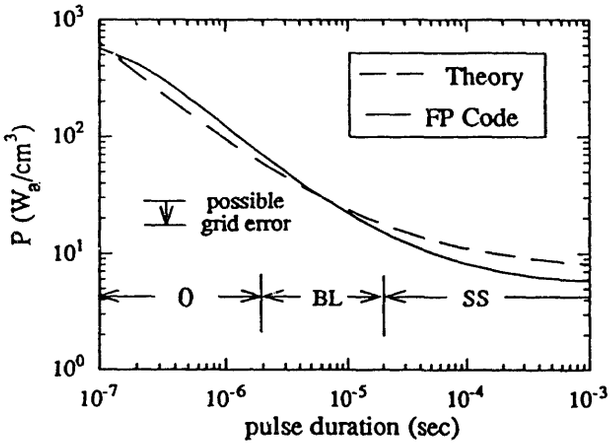

Fig. 2. Comparison of Fokker-Planck-code and analytic results for pulse-averaged absorbed power vs. pulse duration.

m^{-3}, $Z = 1$, $T_e = 25$ keV, $\epsilon_1 = 3.21$, and $\epsilon_2 = 3.92$ corresponding to $\Delta u/u = 0.1$ and parallel index of refraction $N_\parallel = 1.7$. A large, constant diffusion coefficient in the parallel-velocity direction is applied between ϵ_1 and ϵ_2. Flattening of the initially Maxwellian distribution takes place in about 10^{-7} s. After this time, the power is determined by the three terms in Eqs. (1) and (3). These terms each dominate in a different range of τ_p as indicated in the figure. The agreement between the theory and code is good except for long times where the theory over estimates the absorption by about 30%, and where the 1-D and boundary-layer approximations used in the theory are invalid. The overestimate may actually be somewhat larger as the code result tends to decrease somewhat as the number of grid points increases; Fig. 2 was obtained using 160 points in both the speed and pitch-angle coordinates.

As noted earlier, the plateau width is a function of both the power density and the spectral width $\delta N_\parallel$. It is well-approximated by $\left[(\delta N_\parallel/N_\parallel)^2 + (\Delta u/u)_t^2\right]^{1/2}$, where $(\Delta u)_t$ is the trapping width for a single-$N_\parallel$ wave. We obtain $(\Delta u)_t$ by calculating the action enclosed by the separatrix from the electrostatic Hamilton and relating the parallel electric field to $\mathcal{S}$ from the polarization and dispersion relations. The result is

$$(\Delta u/u)_t \cong 1.4\left[\mathcal{S}_\perp(\mathrm{GW/m^2})/N_\parallel\right]^{1/4} A^{-1/8}(G/\mathcal{E}_\parallel)^{1/2}(10\,\mathrm{GHz}/f)^{1/2} \qquad (4)$$

where f is the wave frequency, A is the ion mass in AMU, $G \equiv y^{1/2}(1-y^{-2})^{-1/4}(1+x^2)^{-1/2}$, $x = \omega_{pe}/\omega_{ce}$, $y = \omega/\omega_{lh}$, and ω, ω_{pe}, ω_{ce} and ω_{lh} are, respectively, the wave, electron-plasma, electron-cyclotron, and lower-hybrid frequencies. We have verified Eq. (4) with orbit-code calculations. This width is significant, of order 10%, even for the application of continuous lower-hybrid power at the 50–100 MW level for driving current in the edge of an ITER-like plasma.

RAY TRACING

The opacity for both regimes A and B and the nonlinear plateau width have been incorporated into the ACCOME ray-tracing and current-drive code which was developed within the framework of LLNL-MIT-JAERI collaboration [7]. The code evaluates power deposition as a function of flux surface for model temperature and density profiles and numerically computed equilibria. Additionally, the code provides essential information on the trajectory of rays and the degree of spreading of the $N_\parallel$ spectrum as the rays propagate. We find that, with ITER-like parameters [$n_{e0} = 8 \times 10^{19}$ m^{-3}, $T_{e0} = T_i(0) = 34$ keV, and $B_0 = 4.85$ T, where the subscript 0 denotes on-axis values], rays from plausible launcher locations can pass near the center with acceptable $N_\parallel$, and that, while the mean $N_\parallel$ shifts somewhat, the spectral width remains narrow and nearly constant until the rays pass their distance of closest approach to the plasma center and subsequently broadens. Figure 3 shows a comparison of absorption profiles for a regime

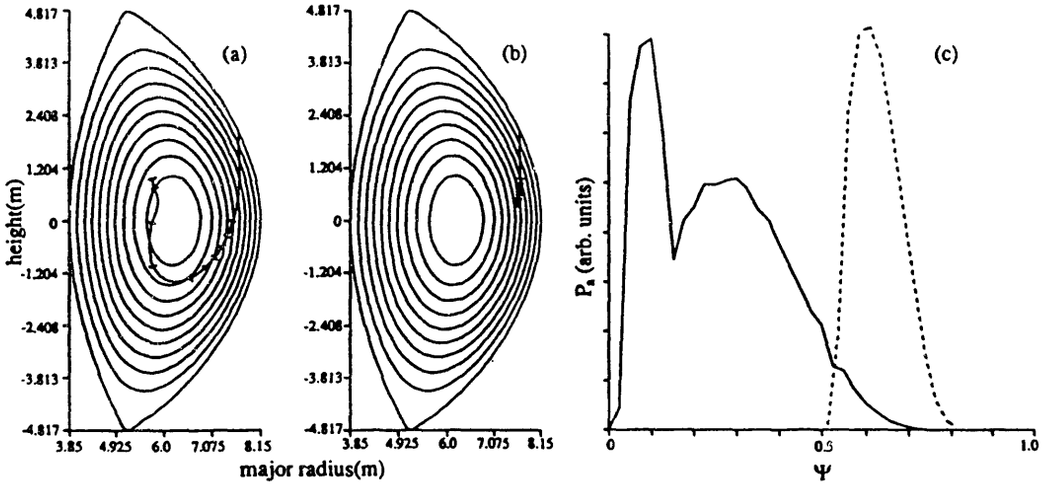

Fig. 3. Comparison of absorption for 9 GW pulsed- and 100 MW continuous-power ITER cases: (a) ray penetration for pulsed case; each tick mark corresponds to absorption of 10 % of the incident power; (b) same for continuous case; (c) power absorbed vs. normalized toroidal magnetic flux Ψ for pulsed (solid curve) and continuous (dashed curve) cases.

B scenario (9 GW, 85 μs, 8 GHz pulses launched with $\delta N_\parallel / N_\parallel = .05$ about $N_\parallel = 1.8$ from 18 m^2 of launcher area; the ray shown is launched from 2 m above the midplane) and a conventional scenario (100 MW continuous power from 2 m^2 launcher area; other parameters the same). The pulsed power penetrates to the core (in fact, to somewhat beyond the center for the chosen parameters) while the continuous power does not. Note that, even though the pulses are much longer and more energetic than those for regime A, the energy per pulse is a small fraction of the plasma energy content, and maintenance of a d.c. current $I \sim$ 10–20 MA would require a repetition period short compared to energy-confinement or current-penetration times. Hence fluctuations in the temperature and current will be small.

Comparable penetration has also been calculated for regime A, but requires an order-of-magnitude higher power density (possibly conflicting with parametric-instability requirements) and long, narrow launchers which follow field lines around the torus. For the sample equilibrium chosen, rays lined up along a field line at the edge of the torus tend to remain so as they propagate inward; hence a launcher elongated along

field lines maps to an r.f. beam elongated along the field in the plasma.

Because the absorption is single-pass and in the high-temperature core of the plasma, the current-drive efficiency should be as given by the narrow-spectrum results of Karney and Fisch (Fig. 3 of Ref. 8). In particular, the momentum-conserving corrections to the test-particle efficiency should be appreciable, yielding efficiencies $\eta = n_e(10^{20}/\mathrm{m}^3)I(\mathrm{A})R(\mathrm{m})/P_a(\mathrm{W}) \gtrsim 0.5$.

The ITER example shown in Fig. 3 is for parameters close to that for the steady-state, engineering-phase scenario of the current ITER Conceptual Design (CDA). We note that the Conceptual Design is not optimized for pulsed-lower-hybrid penetration; in fact, for an alternate high-aspect-ratio design[9] (HARD) now being discussed, comparable penetration can be achieved with less peak power and a smaller launcher area. At 85% of the peak density and temperature for CDA parameters (for steady-state operation: $n_0 = 1.0 \times 10^{20}$ m^{-3}, $T_{e0} = 34$ keV, $B_0 = 4.85$ T, major radius $R = 6.0$ m, minor radius $a = 2.15$ m) we find, for 85 μs, 9 GW, 8 GHz pulses with 18 m^2 launcher area and $\delta N_\parallel/N_\parallel = .05$, that $\alpha^{-}1 = 0.7$ m. We obtain the same result for HARD parameters ($n_0 = 1.7 \times 10^{20}$ m^{-3}, $T_{e0} = 25$ keV, $B_0 = 7.11$ T, $R = 6.33$ m, $a = 1.58$ m) using 3 GW pulses with 6 m^2 of launcher area. Hence for HARD one could plausibly mount launchers in (several) ports as opposed to lining a portion of the wall in between ports.

PARAMETRIC INSTABILITIES

A detailed theoretical investigation of parametric decay instabilities (PDI) has been carried out. The growth rates have been computed numerically using the hot plasma PDI dispersion relationship, valid in the large amplitude regime[10]. The dominant instability is decay into lower-hybrid sideband modes and ion-cyclotron quasi-modes. Convective stabilization can be achieved by restricting the launcher dimensions in the toroidal and/or poloidal directions. We have evaluated the thermal fluctuation level, and obtained the conditions for pump wave depletion. We find that the usual convective threshold power may be increased by a factor of four before pump depletion sets in. Even including this effect, regime A requires a narrow launcher height ($\lesssim 20$ cm) or short pulse length($\lesssim 20$ ns). In regime B the launcher height is increased to 40-60 cm and the width L_z can be ~ 1 m. PDI is most important near the plasma periphery where $T \lesssim 1$ keV and $n \lesssim 2 \times 10^{1^o}$ m^{-3}. Here, the growth rates are largest for modes driven by the parallel electric field of the pump wave, and decay waves are stabilized by Landau damping beyond the separatrix. Considering the finite radial distance between the separatrix and the launcher (~ 10 cm in ITER), we find that pump-wave depletion is avoided for power densities $\lesssim 0.5$ GW/m^2. Furthermore, in at least regime B we estimate that the PDI modes will locally generate a non-Maxwellian distribution, which should heat edge electrons and tend to stabilize the modes by Landau damping. Hence, even without total convective stabilization, we expect a saturated PDI spectrum without causing pump depletion. Experimental results which support this thesis can be found in Ref. 11. We have examined ponderomotive density depletion effects. These should be small ($\Delta n/n \lesssim 0.1$ in regime B). We also consider the scattering of the incoming lower hybrid wave by low frequency background fluctuations. Present estimates indicate acceptably small scattering for the expected fluctuation levels.

SOURCES

There are several options for developing sources appropriate for regime B operation in ITER and reactors, none of which is, however, available at present. Appropriate

source modules would have frequencies in the 5–10 GHz range, peak powers $\gtrsim$ 50 MW and average powers $\gtrsim$ 1 MW with 50 – 100 μsec pulse lengths and $\sim$ 100 Hz repetition rate. The options include gyrotrons, relativistic backward wave oscillators (BWO), cyclotron auto-resonance masers (CARM), and gyroklystrons. Other candidates, such as relativistic klystrons, are ruled out because of the pulse duration requirement.

Gyrotrons have expected efficiencies $\sim$ 25% for operation at $\sim$ 400 kV and 500 A beam current. Disadvantages are low efficiency and the requirement of a complicated mode converter to reduce higher order mode operation to linearly polarized output suitable for lower-hybrid applications. A CARM would use a lower-order mode (like TE_{21}), but the expected efficiency is only about 15%. Unfortunately, to date there is only minimal experience and experimental data available. A BWO could be designed using a TM_{01} mode in a rippled wall, slow wave structure. There is significant high peak-power experience in the USSR which could be adopted to our significant-average-power application. The efficiency expected, however, is in the 20–25% range, similar to that expected for gyrotrons.

The gyroklystron appears to be the most promising concept at the present time. It is similar to the conventional gyrotron but operates at a lower mode (TE_{01}, for example). Therefore application to lower-hybrid schemes is considerably simpler than for gyrotrons. Expected efficiency is if order $\sim$ 30%. Some tunability appears possible. Significant results have been obtained recently at the University of Maryland[13] where power levels of 20 MW, pulse lengths of $\sim$ 1 micro-second, and a gain of 26 dB (with 31% efficiencies) has been achieved at X-band frequencies ($\sim$ 9.87 GHz). More recent, unpublished results indicate[14] that the pulse length has been doubled to $\sim 2\mu$sec, and significantly more gain has been achieved. The low order (TE_{01}) mode used in these experiments is most promising for lower hybrid applications.

EXPERIMENTAL TESTS

Finally, we note that near-term proof-of-principle tests could be done on a number of tokamaks with currently available microwave sources. For this purpose one would deliberately launch waves with high $N_\parallel$ so that the Landau resonance is only moderately far out on the tail of the electron distribution function. For example, for the Microwave Tokamak Experiment MTX, we find, using the modified ACCOME code, that 2 MW, 20 μs, $N_\parallel = 5$, narrow-spectrum pulses at 4.6 GHz from a 640 cm^2 launcher (which would be mounted between ports) can penetrate to the core, while shorter or lower-amplitude pulses, or pulses from a smaller launcher, do not. Parameters for such an experiment would be $n_{e0} \approx 2\text{–}3\times10^{19}$ m^{-3}, $T_{e0} \lesssim 5$ keV, and $B_0 = 5$ T. The table below indicates representative experimental parameters and expected absorption scale lengths α^{-1} for several existing tokamaks (MTX, Versator, DIII), one which is about to become operational (C-Mod), and a proposed upgrade to Versator (Versatile Toroidal Facility, VTF). For all cases, a decrease in peak power, pulse length or launcher area by an order of magnitude decreases α^{-1} by a factor of 3–4. The experiments would attempt to confirm these predictions. One could measure the degree of penetration by looking for the density fluctuations produced by lower hybrid waves (using microwave or optical scattering)[15], or possibly looking for the plateau in the electron distribution function. For all cases, the plateau width ($\sim$ 20–30%) is dominated by nonlinear broadening; hence the results are largely insensitive to $\delta N_\parallel/N_\parallel$ for $\delta N_\parallel/N_\parallel \lesssim 0.1$.

	MTX	Versator	VTF	DIII-D	C-Mod
$n(10^{19}\ \mathrm{cm}^{-3})$	2	0.5	0.4	5	5
$T(\mathrm{keV})$	4	0.4	0.4	4	4
$a(\mathrm{cm})$	16	13	28	67	21
$B(\mathrm{T})$	5	1.2	1.2	2	5
$f(\mathrm{GHz})$	4.6	0.8	0.8	4.6	4.6
$P(\mathrm{MW})$	2	0.1	0.1	2	5
$\tau_p(\mu\mathrm{s})$	20	20	40	40	20
$N_\parallel$	5	12	10	2.9	4
$\delta N_\parallel/N_\parallel$	.02	.1	.05	.05	.05
$A_b(\mathrm{m}^2)$	0.064	0.24	0.24	0.25	0.2
$\alpha^{-1}(\mathrm{cm})$	5.4	9.4	12.6	32	9.5

CONCLUSION

Applying lower hybrid power in short pulses with peak powers in the GW range and durations in the range 50–100 μs significantly enhances the penetration into the core of reactor-grade plasmas, and thus renders lower hybrid waves as a viable means of driving current and heating in the core of a tokamak reactor. It should be possible to avoid significant degradation from parametric instabilities and other competing nonlinear processes. Application to ITER and reactors requires a source-development effort; the gyroklystron appears to be the most promising candidate. However, near-term experimental tests could be done with existing lower-hybrid sources on a number of tokamaks.

ACKNOWLEDGMENTS

This work was performed under the auspices of the U.S. Department of Energy under contract numbers W-7405-ENG-48 at the Lawrence Livermore National Laboratory and DE-AC02-78ET51013 at the Massachusetts Institute of Technology.

REFERENCES

[1] R.S. Devoto, D.T. Blackfield, M.E. Fenstermacher *et al.*, to be published in Nucl. Fusion.
[2] R.H. Cohen, P.T. Bonoli, M. Porkolab and T.D. Rognlien, in Radio-Frequency Power in Plasmas, Eighth Topical Conference, AIP Conf. Proc. **190** (New York, 1989), 126.
[3] R.H. Cohen, T.D. Rognlien, P.T. Bonoli and M. Porkolab, Proc. 13th Int. Conf. on Plasma Physics and Controlled Nucl. Fusion Research (Washington), (IAEA, Vienna, 1991), Vol. 1, p. 805.
[4] A.A. Vedenov, in Reviews of Plasma Physics, M.A. Leontovich, Ed., (Consultants Bureau, New York, 1967) Vol. 3, 229.
[5] N. J. Fisch, Phys. Rev. Lett. **41**, 873 (1978).
[6] R.W. Harvey, M.McCoy and G. Kerbel, Phys. Rev. Lett. **62**, 426 (1989).
[7] P.T. Bonoli, M. Porkolab, J.J. Ramos *et al.*, Nucl. Fusion **30**, 533 (1990).
[9] J.N. Doggett, private communication
[8] C.F. Karney and N.J. Fisch, Phys. Fluids **28**, 116 (1985).
[10] M. Porkolab, Phys. Fluids **20**, 2058 (1977).
[11] M. Porkolab and R.P.H. Chang, Rev. Mod. Phys. **50**, 745 (1978).
[12] Kevin Felch, Varian Assoc., private communication (1990).
[13] W. Lawson et al., Phys. Rev. Lett. **67**, 520 (1991).
[14] R. Tempkin, private communication.
[15] R. Rohatgi *et al.*, Phys. Fluids **3**, 2101 (1991).

END

DATE FILMED

12/04/91